

Carbohydrate-Encapsulated Gold Nanoparticles for Rapid Target-Protein Identification and Binding-Epitope Mapping

Yu-Ju Chen,^{*,[a]} Shu-Hua Chen,^[b] Yuh-Yih Chien,^[b]
Yu-Wan Chang,^[a] Hsin-Kai Liao,^[a] Chih-Yang Chang,^[a]
Mi-Dan Jan,^[a] Ken-Tseng Wang,^[b] and
Chun-Cheng Lin^{*,[a]}

The interactions of cell-surface glycoproteins and glycolipids play important roles in cell–cell communication, proliferation, and differentiation.^[1] Combinations of saccharides, orientations of glycosidic bonds, and branching patterns of linkages allow complex carbohydrates to have a vast diversity of structures for molecular recognition.^[2] Thus, studies of carbohydrate-relat-

ed interactions might provide new insights into their biological roles and reveal new possibilities for drug development.^[3,4] Disclosure of the carbohydrate-recognition sites by X-ray crystallography and NMR spectroscopy has been a challenge due to the difficulty of cocrystallization of targeting proteins and carbohydrates.^[5] At present, most of the binding-epitope analysis methodologies are time-consuming as they screen sets of overlapping peptides spanning a known protein sequence.^[6,7] The advent of an efficient, sensitive, general strategy to identify new carbohydrate-binding lectins and map epitopes is awaited to unravel the complexities of carbohydrate recognition.

Recent developments in mass spectrometry have greatly expanded the possibility of characterizing unknown proteins, including mapping of protein glycosylation sites.^[8] Despite the advantages, the simultaneous characterization of the hundreds to thousands of proteins present in a complex medium still remains a challenge.^[9] However, when mass spectrometry is combined with a biologically active probe to rapidly and specifically target proteins of interest, this targeted proteomic approach can accelerate research for class-specific proteins or biomarkers.^[10] Recently, metal nanoparticles have been used in biological separation and promise to be superior to microbeads.^[11] Furthermore, biomolecule-conjugated gold nanoparticles (AuNPs) are the most popular probes because of their readily assembling with thiolated molecules, their large area/volume ratio for investigating three-dimensional interactions, and their ease of separation by centrifugation.^[12,13] However, the use of functionalized nanoparticles as probes combined with mass spectrometry for carbohydrate–protein recognition studies has not been explored.

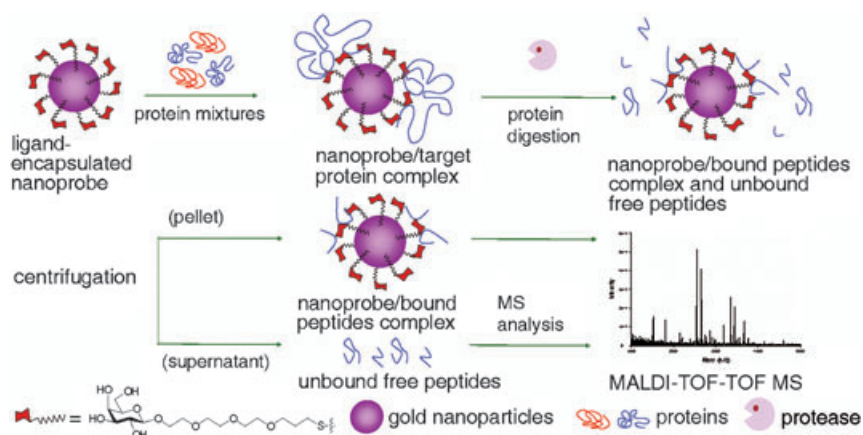
We report here a new approach of using carbohydrate-encapsulated AuNP (c-AuNP) as an affinity probe for the efficient separation and enrichment of target proteins, and then protein identification and epitope mapping by MALDI-TOF MS. The analytical scheme of the approach, nanoprobe-based affinity mass spectrometry (NBAMS), is illustrated in Scheme 1. Unlike other mass spectrometry-based affinity capture approaches that make use of agarose beads^[14] or biochips,^[15] the core component of our scheme is a nanosized biologically active affinity probe. Target proteins can be affinity captured from a mixture by the nanoprobe and directly analyzed on-probe by MALDI-TOF MS. Most significantly, once target proteins have been captured, on-probe digestion followed by removal of unbound peptides allows rapid mapping of carbohydrate-recognition peptide sequences in the proteins.

To demonstrate the general applicability of the NBAMS technique in tackling carbohydrate–protein interactions, proof-of-principle was performed for the specific capture and identification of the galactophilic lectin *Pseudomonas aeruginosa* lectin I (PA-IL) by using c-AuNP. The medium-range affinity ($K_a \sim 3.4 \times 10^4 \text{ M}^{-1}$)^[16] of monomeric D-galactose for PA-IL was enhanced by assembling sugars on nanoparticles. The resulting multivalent interactions^[17] between c-AuNP and PA-IL facilitated highly specific and stable surface affinity separation. To probe the subtle variations in the carbohydrate-binding domain of PA-IL, two carbohydrates—galactose and P^k antigen (Gal α 1→

[a] Dr. Y.-J. Chen, Y.-W. Chang, H.-K. Liao, C.-Y. Chang, M.-D. Jan, Dr. C.-C. Lin
Institute of Chemistry and Genomic Research Center
Academia Sinica Sec. 2
Academia Road, Taipei, 115 (Taiwan)
Fax: (+886) 2-2783-1237
E-mail: yjchen@chem.sinica.edu.tw
cclin@chem.sinica.edu.tw

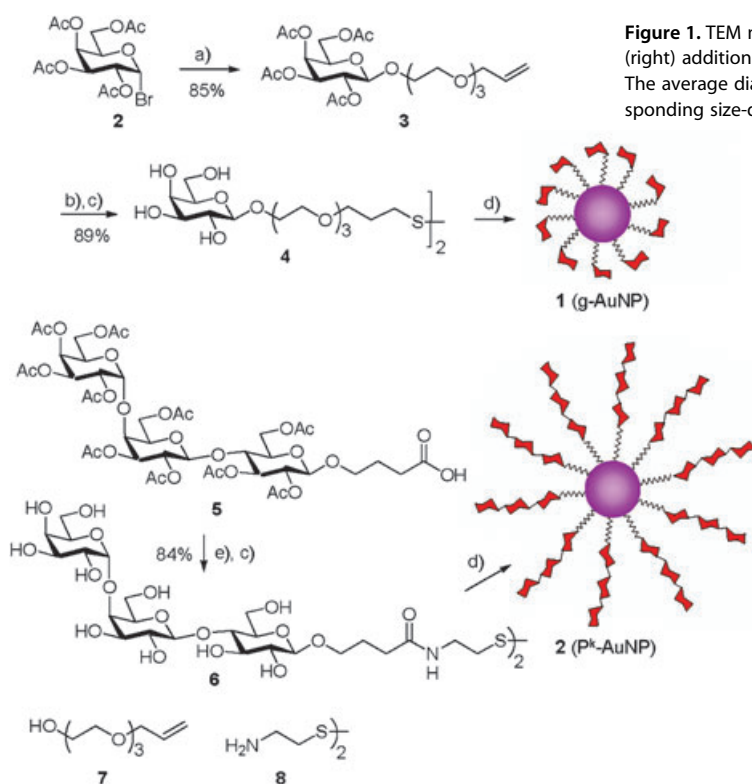
[b] S.-H. Chen, Y.-Y. Chien, Dr. K.-T. Wang
Department of Chemistry, National Taiwan University
Taipei 115 (Taiwan)

Supporting information for this article is available on the WWW under <http://www.chembiochem.org> or from the author.



Scheme 1. The analytical scheme of the NBAMS technique for the specific capture of target proteins and the rapid mapping of binding-epitope-containing peptides.

4Gal β 1 \rightarrow 4Glc; abbreviated as g-AuNP and P^k-AuNP, respectively)—were encapsulated on the gold nanoparticle as shown in Scheme 2. Compound **3** was synthesized by glycosylation of bromide **2** with ethylene glycol acceptor **7** and then treated with thioacetic acid, followed by hydrolysis to give thiogalactosyl dimer **4**.^[18,19] The g-AuNP **1** was prepared by treating HAuCl₄ with **4** in the presence of NaBH₄.^[18,19] The preparation of P^k-AuNP **2** is similar to that of g-AuNP, except that P^k



Scheme 2. Synthesis of g-AuNP (**1**) and P^k-AuNP (**2**). a) **7**, Ag₂CO₃, drierite, CH₂Cl₂, RT, 16 h; b) AcSH, azobisisobutyronitrile, MeOH, 75, 12 h; c) NaOMe (cat), MeOH, RT, 10 min. d) HAuCl₄, NaBH₄. e) **8**, 1-(3-dimethylaminopropyl)-3-ethylcarbodiimide hydrochloride, 1-hydroxy-1*H*-benzotriazole, CH₂Cl₂, RT, 14 h.

dimer **6** was obtained by coupling compound **5**^[20] with cystamine **8**. The average diameter of both AuNPs, determined by TEM, is 4 ± 1 nm (Figure 1). Before addition of PA-1L, the g-AuNPs were dispersed on the grid, whereas intermolecular binding with multivalent PA-1L induced g-AuNP agglutination.

To access the capture specificity and enrichment effect of g-AuNP **1**, the nanoparticles were incubated with a mixture of proteins (PA-1L, enolase, alcohol dehydrogenase, and myoglobin) in

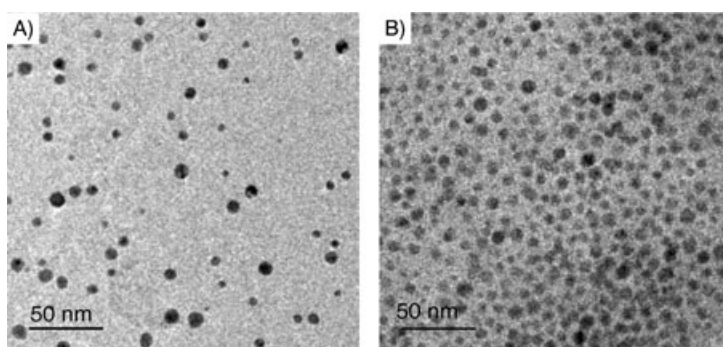


Figure 1. TEM micrographs and size distribution of g-AuNP before (left) and 1 h after (right) addition of 6 μM PA-1L. This image was measured from the agglutinated fraction. The average diameter of AuNPs is 4 ± 1 nm as determined by TEM and from a corresponding size-distribution histogram.

phosphate-buffered saline. After separation of the nanoparticles by centrifugation, the pellet containing g-AuNPs was washed with 25 mM ammonia bicarbonate followed by direct “on-g-AuNP” MALDI-TOF MS analysis. The mass spectrum in Figure 2A reveals the specificity of NBAMS, with a single peak corresponding to PA-1L at $m/z = 12758.8$ (the theoretical average mass is 12762). The clean mass spectrum demonstrates the advantages of NBAMS in providing simultaneous on-g-AuNP protein isolation, enrichment, and sample desalting without the necessity of additional steps. No detectable background peak was observed to arise from the g-AuNP in control experiments (Figure 2B). Figure 2C shows the complex MALDI spectrum of the protein mixture in which the PA-1L was barely observed due to low abundance (4% of molar fraction) and the ion-suppression effect.^[21] Experiments to test the detection sensitivity of the NBAMS approach demonstrated that femtomole concentrations of PA-1L (10 ng mL⁻¹) were readily detectable. A series of dilution experiments of a 100 μL solution (4.7 μM–0.78 nM for the extraction of PA-1L from the protein mixture) were performed,

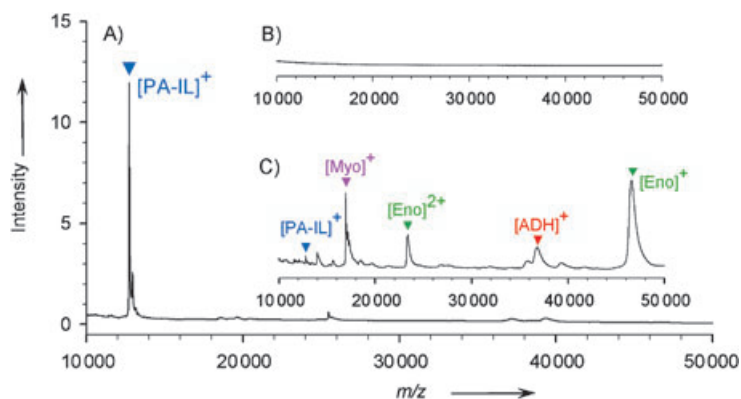


Figure 2. MALDI-TOF mass spectra of specific binding of PA-IL with g-AuNP. A) Selective enrichment and on-g-AuNP clean-up of PA-IL; B) g-AuNP; C) a mixture containing enolase (26 μM), alcohol dehydrogenase (71 μM), myoglobin (1 μM), and PA-IL (5 μM).

and we were able to detect 0.78 nM PA-1L, which is equivalent to 78 fmol of PA-1L (see also Supporting Information).

A major feature of the NBAMS approach is the advantage of on-probe identification of unknown target proteins by mass spectrometry. To confirm the identity of the captured protein, the g-AuNP pellet was subjected to in situ digestion with chymotrypsin. Figure 3A shows the representative peptide mass fingerprinting map of chymotryptic peptides, matched to PA-IL (Swiss-Prot Q05097) in Table 1. Mass spectrometric protein identification provides potential applications in discovering novel receptors and, particularly, the simultaneous identification of multiple class-specific proteins.

To investigate whether the new affinity approach can be a rapid method for probing the noncovalent carbohydrate-binding epitopes of the target protein, the g-AuNP-captured PA-IL was subjected to direct in situ g-AuNP digestion by chymotrypsin without denaturing the native protein structure. Chymotrypsin was chosen because many cleavage sites on the PA-IL sequence can be accessed to generate small proteolytic cleavage products. Thus, carbohydrate-binding sites can be locat-

ed precisely. After centrifugation, the peptides remaining affinity-bound to the g-AuNP were analyzed by MALDI-TOF MS (Figure 3B). The mass spectrum revealed one dominant peak, R83–Y105 (P6) and two minor peaks, A1–Y36 (P14) and R83–S121 (P15); this indicated that at least two discontinuous domains of PA-1L were involved in g-AuNP-specific recognition.

Recently, the high-resolution crystal structure of tetrameric PA-IL with galactose and calcium was reported,^[16] and all the binding residues were observed in the mass spectrum of g-AuNP-bound peptides (Figure 3B). The most intense peak (P6) suggests the position of the relatively strongest binding site, in which three binding residues—Asp100, Val101, and Thr104—are involved in specific galactose recognition. Given the fact that PA-1L has only a moderate

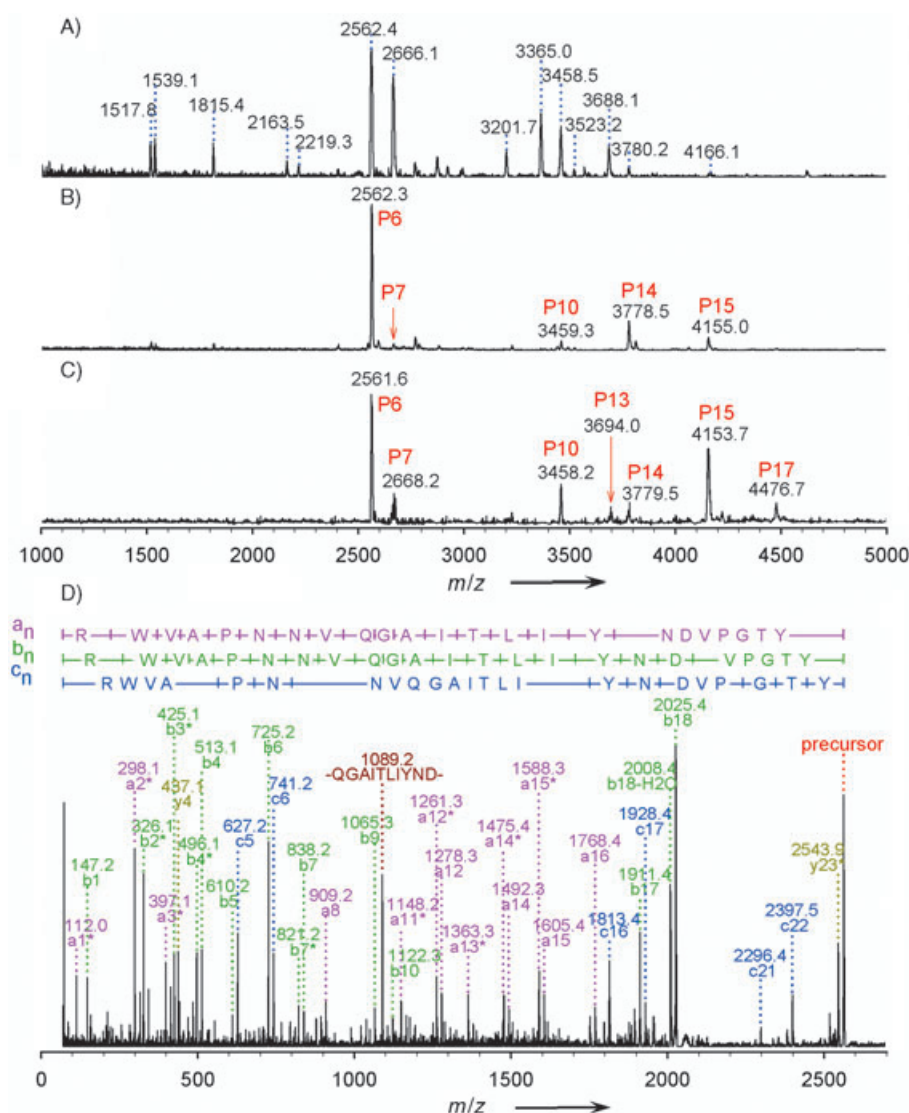


Figure 3. Mapping galactose-binding peptides by protease digestion and the NBAMS technique. A) Peptide mass fingerprinting map of PA-IL captured by g-AuNP. B) MALDI-TOF mass spectrum of the g-AuNP-binding peptides. C) MALDI-TOF mass spectrum of the P⁶-AuNP-binding peptides. D) MS/MS spectrum of the g-AuNP-binding peptide at m/z 2562.3.

Table 1. Masses of observed peptides and corresponding positions in PA-IL sequence.

No.	Theory	Mass (<i>m/z</i>)			Assignment
		Total peptides ^[a]	g-AuNP binding peptides	P ^k -AuNP binding peptides	
P1	1518.7	1517.8	n.d. ^[b]	n.d.	68–82
P2	1539.7	1539.1	n.d.	n.d.	83–96
P3	1816.1	1815.4	n.d.	n.d.	83–98
P4	2164.4	2163.5	n.d.	n.d.	1–20
P5	2220.4	2219.3	n.d.	n.d.	85–105
P6	2562.8	2562.4	2562.3	2561.6	83–105
P7	2667.9	2666.1	2666.2 ^[c]	2668.2	43–67
P8	3201.6	3201.7	n.d.	n.d.	3–33
P9	3365.7	3365.0	n.d.	n.d.	37–67
P10	3458.9	3458.5	3459.3	3458.2	1–33
P11	3522.9	3523.2	n.d.	n.d.	3–36
P12	3687.1	3688.1	n.d.	n.d.	34–67
P13	3694.1	n.d.	n.d.	3694.0	8–42
P14	3780.2	3780.2	3778.5	3779.5	1–36
P15	4155.5	4154.2	4155.0	4153.7	83–121
P16	4167.7	4166.1	n.d.	n.d.	43–82
P17	4478.0	n.d.	n.d.	4476.7	1–42

[a] All peptides after on-g-AuNP or -P^k-AuNP digestion. [b] Not detected. [c] This peptide was only observed after acetonitrile elution of g-AuNP-binding peptides.

affinity for galactose and the shallowness of the binding site,^[16] why the 23-mer peptide (P6) was still bound to the g-AuNP after digestion remains an interesting question. We believe that the immobilization of galactose on AuNPs will increase the ligand surface density and accessibility with a concomitant enhancement in biocapture. The binding of NP with chymotryptic peptides from digestion of free PA-1L was also evaluated; however, g-AuNP showed a lower binding capability with free chymotryptic peptides. The binding of His50/Gln53 and Asn107/Asn108 was observed in the peptides at P7 and P15, respectively. Additionally, the peptide at P14 (the second most intense peak) contains Tyr36, which makes hydrophobic contact with C1 and C2 of galactose.^[16] The unexpected observation of P10 (A1–W33) might be caused by an interaction between the peptide and the poly(ethene glycol) linker. Our results demonstrate that NBAMS is capable of analyzing discontinuous binding epitopes in lectin; this reflects the three-dimensional carbohydrate–protein interaction in solution.

The general capability of the epitope-mapping technique was also tested on the lower-affinity interaction of mannose with Con A ($K_D \sim 10^3 \text{ M}^{-1}$).^[22] The results were also in good agreement with the literature (unpublished data).

It has been reported that the binding affinity of galactoside (Gal) with PA-1L showed the descending order of P^k antigen > α -monogalactoside > β -monogalactoside.^[23] The different binding epitopes of PA-IL with the α -galactoside-containing trisaccharide P^k were examined. Figure 3C shows that the P^k-AuNP binding peptides were similar to those of g-AuNP; this suggests that P^k-AuNP interacts with PA-IL mainly through the terminal Gal of the P^k antigen. Compared with the g-AuNP binding peptides, the major differences include the appearance of

two peptides A8–W42 (P13) and A1–W42 (P17), and the increased relative intensities of three peptides, G43–M67 (P7), A1–W33 (P10), and R83–S121 (P15). These might be due to a subtle change in the orientation of the α -Gal of the P^k antigen that results in enhanced binding affinity of PA-IL with Gal. These results clearly demonstrated that the NBAMS approach can reflect the change of interaction modes with different carbohydrates. Finally, the advantage of mass spectrometry as a readout for peptide sequencing is shown in the MALDI-MS/MS spectrum of the bound peptide (P6), which depicts several fragment ion series,^[24] a_n, b_n, and c_n (Figure 3D), that confirmed the sequence of the peptide R83–Y105 bound to galactose.

In summary, we have demonstrated the feasibility of carbohydrate-functionalized nanoprobe for the simultaneous enrichment and isolation of target proteins from a mixture at the femtomole level, and subsequent protein identification and mapping of the binding-epitope-containing peptides with minimum sample handling. Given the flexibility and ease of adapting functionalized nanoprobe to ligand-fishing of class-specific proteins, the rapid NBAMS approach shows promise in profiling the proteome in a specific binding-dependent manner. The effective identification of ligand-binding epitopes will provide a wealth of information for understanding ligand–receptor recognition.

Acknowledgements

We acknowledge financial support from Academia Sinica and the National Science Council, Taiwan. We thank the High-Throughput Facilities for Proteomic Research for the use of TOF-TOF MS, Dr. H.-M. Lin for TEM measurements, and Prof. Sunney I. Chan for comments on the work.

Keywords: carbohydrates • gold • glycosylation • mass spectrometry • nanoparticles • proteomics

- [1] C. R. Bertozzi, L. L. Kiessling, *Science* **2001**, *291*, 2357.
- [2] D. M. Ratner, E. W. Adams, M. D. Disney, P. H. Seeberger, *ChemBioChem* **2004**, *5*, 1375.
- [3] B. P. Rempel, H. C. Winter, I. J. Goldstein, O. Hindsgaul, *Glycoconjugate J.* **2002**, *19*, 175.
- [4] T. Feizi, F. Fazio, W. Chai, C. H. Wong, *Curr. Opin. Struct. Biol.* **2003**, *13*, 637.
- [5] M. R. Wormald, A. J. Petrescu, Y. L. Pao, A. Glithero, T. Elliott, R. A. Dwek, *Chem. Rev.* **2002**, *102*, 371.
- [6] E. K. Lau, C. D. Paavola, Z. Johnson, J. P. Gaudry, E. Geretti, F. Borlat, A. J. Kungl, A. E. Proudfoot, T. M. Handel, *J. Biol. Chem.* **2004**, *279*, 22 294.
- [7] M. D. Abd-Alla, T. F. Jackson, G. C. Soong, M. Mazanec, J. I. Ravdin, *Infect. Immun.* **2004**, *72*, 3974.
- [8] S.-I. Nishimura, K. Niikura, M. Kuroguchi, T. Matsushita, M. Fumoto, H. Hinou, R. Kamitani, H. Nakagawa, K. Deguchi, N. Miura, K. Monde, H. Kondo, *Angew. Chem.* **2005**, *117*, 93; *Angew. Chem. Int. Ed.* **2005**, *44*, 91.
- [9] J. D. Wulfkühle, L. A. Liotta, E. F. Petricoin, *Nat. Rev. Cancer* **2003**, *3*, 267.
- [10] J. L. Bundy, C. Fenselau, *Anal. Chem.* **2001**, *73*, 751.
- [11] C. Xu, K. Xu, H. Gu, X. Zhong, Z. Guo, R. Zheng, X. Zhang, B. Xu, *J. Am. Chem. Soc.* **2004**, *126*, 3392.
- [12] J. M. de la Fuente, A. G. Barrientos, T. C. Rojas, J. Rojo, J. Cañada, A. Fernández, S. Penadés, *Angew. Chem.* **2001**, *113*, 2317; *Angew. Chem. Int. Ed.* **2001**, *40*, 2257.
- [13] E. Katz, I. Willner, *Angew. Chem.* **2004**, *116*, 6166; *Angew. Chem. Int. Ed.* **2004**, *43*, 6042.

- [14] F. Ciruela, J. Burgueno, V. Casado, M. Canals, D. Marcellino, S. R. Goldberg, M. Bader, K. Fuxe, L. F. Agnati, C. Lluís, R. Franco, S. Ferre, A. S. Woods, *Anal. Chem.* **2004**, *76*, 5354.
- [15] B. T. Houseman, M. Mrksich, *Chem. Biol.* **2002**, *9*, 443.
- [16] G. Cioci, E. P. Mitchell, C. Gautier, M. Wimmerova, D. Sudakevitz, S. Perez, N. Gilboa-Garber, A. Imberty, *FEBS Lett.* **2003**, *555*, 297.
- [17] M. Mammen, S. K. Choi, G. M. Whitesides, *Angew. Chem.* **1998**, *110*, 2908; *Angew. Chem. Int. Ed.* **1998**, *37*, 2754.
- [18] C.-C. Lin, Y.-C. Yeh, C.-Y. Yang, C.-L. Chen, G.-F. Chen, C.-C. Chen, Y.-C. Wu, *J. Am. Chem. Soc.* **2002**, *124*, 3508.
- [19] C.-C. Lin, Y.-C. Yeh, C.-Y. Yang, G.-F. Chen, Y.-C. Chen, Y.-C. Wu, C.-C. Chen, *Chem. Commun.* **2003**, 2920.
- [20] S.-Y. Hsieh, M.-D. Jan, L. N. Patkar, C.-T. Chen, C.-C. Lin, *Carbohydr. Res.* **2005**, *340*, 49.
- [21] R. Knochenmuss, R. Zenobi, *Chem. Rev.* **2003**, *103*, 441.
- [22] K. Shimura, K. Kasai, *Anal. Biochem.* **1995**, *227*, 186.
- [23] B. Lanne, J. Ciopraga, J. Bergstrom, C. Motas, K. A. Karlsson, *Glycoconjugate J.* **1994**, *11*, 292.
- [24] P. Roepstorff, J. Fohlman, *Biomed. Mass Spectrom.* **1984**, *11*, 601.

Received: January 20, 2005

Published online on May 25, 2005